

Northumbria Research Link

Citation: Burhan, Muhammad, Shahzad, Muhammad Wakil and Ng, Kim Choon (2018) Hydrogen at the rooftop: Compact CPV-hydrogen system to convert sunlight to hydrogen. Applied Thermal Engineering, 132. pp. 154-164. ISSN 1359-4311

Published by: Elsevier

URL: <https://doi.org/10.1016/j.applthermaleng.2017.12.0...>
<<https://doi.org/10.1016/j.applthermaleng.2017.12.094>>

This version was downloaded from Northumbria Research Link:
<http://nrl.northumbria.ac.uk/id/eprint/42234/>

Northumbria University has developed Northumbria Research Link (NRL) to enable users to access the University's research output. Copyright © and moral rights for items on NRL are retained by the individual author(s) and/or other copyright owners. Single copies of full items can be reproduced, displayed or performed, and given to third parties in any format or medium for personal research or study, educational, or not-for-profit purposes without prior permission or charge, provided the authors, title and full bibliographic details are given, as well as a hyperlink and/or URL to the original metadata page. The content must not be changed in any way. Full items must not be sold commercially in any format or medium without formal permission of the copyright holder. The full policy is available online: <http://nrl.northumbria.ac.uk/policies.html>

This document may differ from the final, published version of the research and has been made available online in accordance with publisher policies. To read and/or cite from the published version of the research, please visit the publisher's website (a subscription may be required.)



**Northumbria
University**
NEWCASTLE



UniversityLibrary

Hydrogen at the Rooftop: Compact CPV-Hydrogen system to Convert Sunlight to Hydrogen

Muhammad Burhan¹, Muhammad Wakil Shahzad¹, Ng Kim Choon¹

¹Water Desalination and Reuse Center (WDRC), Biological and Environmental Science & Engineering (BESE), King Abdullah University of Science and Technology, Thuwal 23955-6900, Saudi Arabia

Email: muhammad.burhan@kaust.edu.sa; muhammad.shahzad@kaust.edu.sa; kimchoon.ng@kaust.edu.sa

Abstract

Despite being highest potential energy source, solar intermittency and low power density make it difficult for solar energy to compete with the conventional power plants. Highly efficient concentrated photovoltaic (CPV) system provides best technology to be paired with the electrolytic hydrogen production, as a sustainable energy source with long term energy storage. However, the conventional gigantic design of CPV system limits its market and application to the open desert fields without any rooftop installation scope, unlike conventional PV. This makes CPV less popular among solar energy customers. This paper discusses the development of compact CPV-Hydrogen system for the rooftop application in the urban region. The in-house built compact CPV system works with hybrid solar tracking of 0.1° accuracy, ensured through proposed double lens collimator based solar tracking sensor. With PEM based electrolyser, the compact CPV-hydrogen system showed 28% CPV efficiency and 18% sunlight to hydrogen (STH) efficiency, for rooftop operation in tropical region of Singapore. For plant designers, the solar to hydrogen production rating of 217 kWh_e/kg_{H₂} has been presented with 15% STH daily average efficiency, recorded from the long term field operation of the system.

Keywords: CPV, Hydrogen, Solar to Hydrogen, Concentrated Photovoltaic, Solar Cell.

1. Introduction

In current alarming situation of greenhouse gas emissions, global warming is drastically affecting the environment [1-4]. Use of renewable energy resources as primary energy supply is the only solution for sustainable future [5-8]. Among all of the energy sources, solar energy has the highest energy potential that is many times higher than the current global energy demand [9-11]. On the other hand, solar energy is only available during diurnal period, but with intermittent supply [12]. In order to compete with the conventional fossil fuel based power plants, the sustainable energy source must also be able to provide steady power supply with high energy density [13]. However, due to solar intermittency, there is a need for energy storage system for steady power supply [14].

The simplest method of solar energy utilization is its conversion into electricity through solar cell. Although, conventional single junction solar cells are having 99% share in current photovoltaic market [15], but they do not offer the highest efficiency. The multi-junction solar

38 cell (MJC) provides highest efficiency of 46% [16] which is 2-3 times higher than the
39 conventional single junction cells [17]. However, due to higher material cost, they are utilized
40 as concentrated photovoltaic (CPV) system [18]; highly efficient photovoltaic technology of
41 the time.

42 Despite highest efficiency, CPV technology is only having a minor share in the photovoltaic
43 market [19]. Conventional gigantic design of CPV unit is the main reason of its limited
44 application scope [20,21], which is only suitable and targeted for the open desert field operation
45 as CPV can only respond to beam radiation of solar energy [22]. For that, it tracks sun
46 movement during its operation. On the other hand, the conventional single junction flat plate
47 PV system has significant share of its installations as rooftop system. Currently, most of the
48 countries are planning to increase the rooftop installations of PV systems to 40-50% of their
49 total capacity [23]. Contrariwise, CPV technology appeared to be unattractive with less
50 customers due to its limited application scope as it is only available as gigantic units. Therefore,
51 there is a need to have a compact system design which should not only eliminate the installation
52 related restriction of CPV but it should also be easily available for the customers of each
53 capacity level.

54 Although, CPV system can convert solar radiations into electricity, a high grade energy, with
55 highest efficiency but it still remains intermittent due to unsteady availability of solar radiations
56 [24]. Conventional electrochemical energy storage i.e. battery can only provide a feasible and
57 economical solution when the need is for short term energy storage and for a small capacity
58 system [25]. In order to be a primary energy source, there is a need to have long term energy
59 storage capability of 10-20 years, with high power density [26]. Electrolytic hydrogen
60 production from water splitting, not only provides a sustainable long term energy storage
61 option but also an alternate sustainable fuel with high power density [27]. It can not only be
62 converted back into electricity when needed, using fuel cell, but it can also be exported as a
63 fuel where it is needed [28]. Therefore, with compact CPV system, such technology will not
64 only be in the reach of every customer but by coupling it with electrolytic hydrogen system, a
65 sustainable and highly efficient energy source will be available at the rooftop of every
66 commercial or housing building. The main restriction for the compact CPV design is the
67 development of cost effective and highly accurate solar tracking system. In addition, for
68 compact CPV system, larger number of solar tracking units are needed and due to highly
69 accurate solar tracking requirements, the overall cost of system increases for the same capacity.
70 Therefore, this demands to develop a cost effect but highly accurate and compact tracking unit
71 for compact CPV design. Moreover, all of the commercially available solar tracking sensors,
72 with tracking accuracy as of CPV standard, cannot provide an economical solution due to their
73 high capital cost [29,30] as more number of units are needed for the compact CPV system
74 design.

75 In this paper, a prototype of compact CPV-hydrogen system is designed, developed and tested
76 for rooftop application. A compact solar tracking system is developed with highly accurate,
77 low cost, novel solar tracking sensor and microcontroller based control. On the other hand, as
78 CPV systems are only considered to be suitable for open desert field regions with high DNI
79 availability, therefore, the performance of developed CPV-hydrogen system is also tested for

80 urban rooftop application in tropical environment. The system was installed at the rooftop of
81 EA building at NUS Singapore. It showed maximum sunlight to hydrogen (STH) efficiency of
82 18% which is not only 4 times higher than the conventional PV-hydrogen system (i.e. PV
83 efficiency of 7.5% [31] and electrolyser efficiency of 68% [32]) but it is also two times higher
84 than the electrical efficiency of PV system alone. The developed system showed daily average
85 STH efficiency of 15% and STH production rating of 217 kWh/kg. Such proposed system will
86 not only introduce a highly efficient photovoltaic system for everyone but also a sustainable
87 energy source with steady power supply.

88 **2. Compact CPV-Hydrogen System Design and Scope**

89 The conceptual representation of compact CPV-Hydrogen system is shown in Fig. 1. The
90 overall system has two sub-components i.e. CPV system and hydrogen production/re-
91 utilization/storage system. In current study, the main focus is the development of compact CPV
92 system that will not only eliminate its installation restrictions but it will also provide CPV the
93 same application scope as that of conventional PV i.e. operation at the rooftop of residential or
94 commercial buildings. However, by utilizing such compact CPV system, a highly efficient
95 prototype of CPV-hydrogen system will be developed and tested for its operation under tropical
96 weather conditions of Singapore. The excess electrical power produced by the CPV will be
97 converted into hydrogen/oxygen by electrolytic splitting of water molecule. Such produced
98 hydrogen can not only be converted back into electricity when needed, using fuel cell, but it
99 can also be transported to other places as a fuel where it can be directly burnt or converted back
100 into electricity. Such compact CPV-hydrogen system will not only boost the market share of
101 highly efficient CPV system with steady power supply and broader application scope, but it
102 will also provide a sustainable power source at the rooftop of each housing unit. Beside power
103 production system, such solar energy system can also be used for sustainable hydrogen and
104 oxygen production for process use in industries. However, oxygen can be used as an industrial
105 disinfecting agent, after converting into ozone.

106 The CPV system can be further split up into two systems i.e. CPV module, consisting of optical
107 assembly of lenses or reflectors with the multi-junction solar cell (MJC), and solar tracking
108 unit. Current compact CPV system design focuses on the design of solar tracking units. Due to
109 larger number of tracking units needed for compact CPV design, the tracking unit must be
110 simple and cost effective. Fig. 2 shows the design schematic of compact CPV unit and proposed
111 solar tracking sensor. As shown, the CPV unit consists of two axis solar tracker, onto which
112 the CPV module is mounted. Solar tracking system can be further divided into its mechanical
113 assembly and control circuit. The mechanical assembly provides support structure and
114 mechanical drive, consisting of worm gear and wheel. On the other hand, the control circuit is
115 based upon the motor drivers and the central microcontroller that controls and defines the solar
116 tracker movement. The solar tracking system needed for CPV system is different than that of
117 the conventional PV systems. CPV systems require tracking accuracy of order 0.1° - 0.3° which
118 is about 10-100 times higher than that of conventional PV tracking units. If such high tracking
119 accuracy is not achieved then the CPV power output can drop from maximum to zero. In order
120 to ensure high tracking accuracy, hybrid tracking algorithm is utilized for the proposed compact
121 CPV unit.

122

123 The hybrid tracking algorithm is based upon both passive (astronomical) and active (optical)
124 tracking algorithms. The passive tracking algorithm utilizes predefined solar geometry model
125 [33] to determine the sun position at any place and any time of the day. Azimuth and zenith are
126 two tracking angles which define the sun position in horizontal and vertical planes,
127 respectively. The azimuth angle ' θ_a ' is referenced from south in horizontal plane. However, the
128 zenith angle ' θ_z ' is referenced from horizontal level, in vertical plane. Both zenith and azimuth
129 angles are given by equations (1) and (2A) or (2B), respectively.

130
$$\theta_z = \cos^{-1}\{\sin \phi \sin \delta + \cos \phi \cos \delta \cos \omega\} \quad (1)$$

131 If $\omega > 0$,

132
$$\theta_a = 360 - \left[90 + \cos^{-1} \frac{\sin \delta - \sin(90 - \theta_z) \sin \phi}{\cos(90 - \theta_z) \cos \phi} \right] \quad (2A)$$

133 If $\omega < 0$,

134
$$\theta_a = 90 + \cos^{-1} \frac{\sin \delta - \sin(90 - \theta_z) \sin \phi}{\cos(90 - \theta_z) \cos \phi} \quad (2B)$$

135 where ' ω ', ' δ ' and ' ϕ ' are hour angle, declination angle and latitude, respectively. The passive
136 or astronomical tracking algorithm works as per defined solar position. However, in such case
137 the tracking accuracy cannot be ensured as astronomical tracking is based upon open loop
138 configuration, with no feedback. The mechanical drive is prone to backlash which can easily
139 introduce tracking error. Therefore, in order to ensure required tracking accuracy, there is a
140 need for real time feedback from solar tracking sensor, regarding solar position.

141 Fig. 2 shows the design and arrangement of proposed double lens collimator based solar
142 tracking sensor. The solar tracking sensor is based upon two parts. First one is the optical
143 assembly that amplifies the solar radiations and directs the resultant beam to an array of
144 photosensors, which provides the required feedback in form of electrical signal. The optical
145 collimator is based upon a certain arrangement of convex and concave lenses, sharing same
146 focal point. The parallel solar rays, after passing through collimator, are converted into a
147 concentrated form of collimated beam. The convex lens converges the parallel rays at its focal
148 point. However, the concave lens, placed in the path of these converging rays, makes them
149 parallel again as both lenses share the same focal point. Such concentrated but collimated beam
150 is then directed at the centre of photosensor array, appearing as a concentrated bright spot.
151 During operation, the solar tracking sensor is aligned with the tracker position such that when
152 tracker is accurately facing towards the sun, the concentrated bright spot is exactly in the centre
153 of photosensors array. In case of tracking error, the solar radiations, received by the solar
154 tracking sensor, do not remain parallel to its optical axis. As a result of this misalignment, the
155 concentrated bright spot deviates from its centre position. When the tracking error exceeds
156 from tracking limit, the deviation of bright spot increases to such an extent that it hits any of
157 the photosensor in the array. In this case, a feedback signal is generated by the corresponding

158 photosensor, which is translated by the control circuit of solar tracker as a tracking error.
 159 According to the position of each of the photosensor in the array, the microcontroller is
 160 programmed in such a way that it moves trackers accordingly, so that the bright spot again
 161 comes in the centre of photosensors array. As far as the concentrated bright spot remains inside
 162 the photo-sensor array, the tracker is assumed to be accurately tracking the sun within the
 163 defined error limits. The distance ‘S’ between convex and concave lenses, and the thickness of
 164 concentrated collimated beam ‘b_t’ can be calculated by equations (3) and (4), respectively.

$$165 \quad S = f_{cx} + (-f_{cn}) \quad (3)$$

$$166 \quad b_t = \frac{D_{cx}}{f_{cx}} \bullet f_{cn} \quad (4)$$

167 The ray tracing simulation of proposed solar tracking sensor is also shown at the right side of
 168 Fig. 2. It can be seen that a perfect collimated beam can be obtained after concave lens. It must
 169 be noted that the distance between concave lens and photosensor array defines the sensitivity
 170 of solar tracking sensor. In addition, the distance among the photosensors in the array defines
 171 the error limit of the solar tracking unit.

172 As mentioned before, the movement of the solar tracker is managed by the control box which
 173 generates the required tracking signals, according to the hybrid tracking algorithm. For
 174 compact CPV system design, such control box must simple, robust and cost effective so that it
 175 can be easily implemented with required accuracy of CPV system. A simple schematic of
 176 microcontroller based control box for compact CPV system, is shown in Fig. 3. The heart of
 177 the control box is the microcontroller that implements the hybrid tracking algorithm and
 178 controls the tracker movements accordingly. The GPS and real time clock (RTC) modules are
 179 used to get the required information of date, time, latitude and longitude of particular location,
 180 to implement the astronomical tracking algorithm. On the other hand, the solar tracking sensor
 181 is connected to microcontroller through ADC (analogue to digital converter) communication,
 182 to convert its analogue feedback signal into a digital signal so that it can be read and
 183 implemented by the microcontroller. Based upon the required tracking information, the tracker
 184 movement is controlled by sending signals to the motor drivers.

185

186 **3. Developed CPV-Hydrogen System and Testing Methodology**

187 According to the proposed design of compact CPV system, as demonstrated in the previous
 188 section, a working prototype of compact CPV-hydrogen system is developed at the rooftop of EA
 189 building in NUS Singapore. The developed prototype is shown in Fig. 4.

190 The developed CPV system is based upon a CPV module, utilizing 2x2 Fresnel lens array and
 191 triple junction InGaP/InGaAs/Ge solar cell. The CPV module is mounted onto the mechanical
 192 structure of compact two axis solar tracking unit. For the developed system, the gear ratio of 40 is
 193 implemented for azimuth driving assembly and gear ratio of 60 is implemented for zenith driving
 194 assembly. The high gear ratio for zenith axis is due to the high torque requirement as the weight

195 of CPV module is supported by the zenith driving assembly. Therefore, by utilizing the stepper
196 motor of resolution 1.8°/step and stepper motor driver of ratio ‘16’, the azimuth and zenith driving
197 assemblies have resolution of 0.0028125° and 0.001875° per step, respectively as given by
198 equation (5).

$$\text{Tracker Movement/Step} = \frac{\text{Motor Step}}{\text{Driver Step} \times \text{Gear Ratio}} \quad (5)$$

200 The developed control box for such a tracking system is also shown in Fig. 4. The hybrid tracking
201 algorithm is developed in C-programming and compiled through codevisionAVR. A prototype of
202 solar tracking sensor is also developed and connected to the microcontroller through ADC
203 communication. The developed tracker is designed to have error sensing capability of as low as
204 0.1°. In hybrid tracking algorithm, the astronomical tracking acts as the main tracking method.
205 However, when such passive tracking algorithm completes then the feedback from solar tracking
206 sensor is obtained. If the feedback signal is low then this indicates that the tracker is accurately
207 facing towards the sun. However, in case of high feedback signal, the tracker is adjusted such that
208 the feedback signal drops to zero again. After ensuring the tracking accuracy through feedback
209 signal, the hybrid tracking algorithm starts again and remains continued during the operation.

210 During CPV operation, the solar tracking system ensures that the Fresnel lens along with the whole
211 CPV module, is facing towards the sun, within their acceptable optical error limit. The beam solar
212 radiations, after passing through Fresnel lens, are converged at the inlet aperture of glass
213 homogeniser which further directs and uniformly distributes them over the MJC area. The multi-
214 junction cell, placed at the outlet aperture of glass homogeniser, converts the received solar
215 radiations into electrical power. However, some of the energy is lost as heat which is dissipated
216 through heat spreader and heat sink, place at the back side of MJC. The power output of CPV
217 system is then supplied to the PEM electrolyser based hydrogen production unit, through MPPT
218 (maximum power point tacking) device or DC-DC converter. PEM electrolyser has its own
219 current-voltage (I-V) characteristics, which depend upon the amount of current flowing through
220 the circuit. On the other hand, the solar cell has a certain operating point with maximum efficiency,
221 at certain concentration. Therefore, for overall maximum system efficiency, it is very important
222 for both of the units that they must operate at their optimum points.

223 The hydrogen production system is based upon a small stack of PEM electrolyzers, where
224 produced CPV electricity is used to split water into hydrogen and oxygen. The produced
225 hydrogen/oxygen gases are then stored into cylinders for storage and further used. For this
226 purpose, a mechanical compression system is developed, which not only compresses the produced
227 gases into the storage cylinders but also helps to have the flow of gases through the production
228 unit. The flow schematic of developed compact CPV-hydrogen system is shown in Fig. 5. All of
229 the feedback signals from the system, either system production or sensor output, are recorded
230 through central data logging unit, to analyse the system performance. In order to measure the
231 quantity of produced gases, they are first stored temporarily over the water and by the amount of
232 water displaced, as measured through level sensor of ±1.5% accuracy, the quantity of produced
233 gases is determined. Moreover, for testing and prototyping purpose, only single compressor is
234 used for the storage of both types of gases, due to limited budget. However, in such case, proper

235 flushing of line is required before switching the compressor to other gas supply mode, to avoid
 236 mixing of gases in the system.

237 The performance of the developed system is measured in terms of its power output and energy
 238 efficiency. The performance parameters which are measured for the system performance analysis,
 239 are given by equations (6) to (10).

$$240 \quad P_{CPV} = V_{CPV} \times I_{CPV} \quad (6)$$

$$241 \quad \eta_{CPV} = \frac{P_{CPV}}{DNI \times A_{con}} \quad (7)$$

$$242 \quad n_{E,H2} = \eta_{EF} \frac{N_{EC} I_E}{n_E F} \quad (8)$$

$$243 \quad \eta_{EL} = \frac{n_{E,H2} \cdot 237200}{I_E \cdot U_E} = \frac{\eta_{EF} \cdot 1.23}{U_E} \quad (9)$$

$$244 \quad \eta_{CPV_H2} = \eta_{CPV} \cdot \eta_{EL} \quad (10)$$

245 Where ‘ V_{CPV} ’ and ‘ I_{CPV} ’ are voltage and current output of CPV system, respectively and their
 246 product gives the total CPV power output ‘ P_{CPV} ’, as given by equation (6). The efficiency of CPV
 247 ‘ η_{CPV} ’ is given by the ratio of input to output power i.e. equation (7). Here, DNI (Direct Normal
 248 Irradiance) represents the amount of solar beam radiations received by the CPV system, measured
 249 in W/m^2 using Eppleylab Pyrheliometer with $\pm 1\%$ calibrated accuracy, and ‘ A_{con} ’ gives the
 250 receiver area of Fresnel lens array. For electrolyser, the amount of hydrogen produced ‘ $n_{E,H2}$ ’ is
 251 given by the equation (8) where ‘ n_E ’ represents the number of electrons needed for the electrolysis,
 252 ‘ F ’ represents the Farady constant, ‘ N_{EC} ’ represents the number of electrolyser cells connected in
 253 series, ‘ η_{EF} ’ represents the Farady efficiency and ‘ I_E ’ represent the current flowing through the
 254 electrolyser. The efficiency of electrolyser ‘ η_{EL} ’ is solely depending upon its operating voltage
 255 ‘ U_E ’, as given by (9). The numerator of equation (9) gives the energy output in form of hydrogen
 256 as 237200 J/mol represent the Gibbs free energy of water electrolysis reaction, which is equivalent
 257 to 1.23V, called as thermos-neutral voltage. The overall STH efficiency of CPV-hydrogen system
 258 ‘ η_{CPV_H2} ’ is then given by the equation (10), which is the product of efficiencies of both units i.e.
 259 CPV and Electrolyser.

260 However, the efficiency of conventional PV system is based upon the global horizontal
 261 irradiance (GHI). Therefore, in case of PV, the STH can be calculated as.

$$262 \quad \eta_{PV} = \frac{P_{PV}}{GHI \times A_{con}} = \frac{V_{PV} \times I_{PV}}{GHI \times A_{con}} \quad (11)$$

$$263 \quad \eta_{PV_H2} = \eta_{PV} \cdot \eta_{EL} \quad (12)$$

264 4. Results and discussion

265 Before analysing the overall performance of developed compact CPV-hydrogen system, the
266 individual performance of CPV and electrolyser units is evaluated. Fig. 6 shows the maximum
267 performance of developed CPV system, in form of conversion efficiency with heat sink
268 temperature and received DNI, during different times of the day. It can be seen that the CPV
269 system showed maximum solar energy conversion efficiency of 28%. However, the CPV
270 efficiency slightly dropped to 25-26% in the noon time despite increase in the received DNI. Such
271 drop in the efficiency is due to increase in the cell temperature which can be seen through increase
272 in the heat sink temperature. With increase in the DNI, concentration at the cell area increases,
273 resulting in more heat loss and consequently, the system efficiency drops slightly.

274 Fig. 7 shows the performance characteristics of PEM electrolyser used in the development of
275 current system. Each data point is based upon the average value of five experimental data sets
276 repeated under similar conditions. In addition, the measured experimental data set has uncertainty
277 of $\pm 0.42\%$ and confidence level of 98% for current, uncertainty of $\pm 0.43\%$ and confidence level
278 of 98% for voltage and uncertainty of $\pm 0.97\%$ and confidence level of 95% for gas flow
279 measurement. Therefore, Faraday efficiency has uncertainty of $\pm 1.39\%$. From the I-V
280 characteristics of the electrolyser, it can be seen that the electrolytic reaction is starting after 1.4 V
281 and then a proportional trend can be seen between current and voltage of electrolyser. On the other
282 hand, if we look at the Faraday efficiency of PEM electrolyser unit, it is almost 100% throughout
283 the range of operating voltage. Thus, equation (8) can also be used to calculate the instantaneous
284 production of hydrogen, other than the gas quantity measurement system developed for this setup.
285 Similar to the I-V characteristics of the electrolyser, its hydrogen production is also proportional
286 to the operating voltage. However, higher operating voltage can reduce the system efficiency, as
287 given by equation (9), because Faraday efficiency is almost 100% for the complete range of
288 operating voltage. Therefore, for larger gas production with high system efficiency, the slope of
289 hydrogen production versus voltage graph must be higher instead of operating the system at higher
290 voltage.

291 In order to analyse the performance variation of CPV-hydrogen system under real field condition,
292 the system was operated for the whole day operation and the system performance curves are
293 shown in Fig. 8. It must be noted that the DNI data was measured with uncertainty of $\pm 1\%$ and
294 confidence level of 96%. On the other hand, CPV voltage and current measurements have
295 uncertainties of $\pm 0.46\%$ and $\pm 0.49\%$, respectively with 97% confidence level. Therefore, the
296 uncertainties in the CPV efficiency, electrolyser efficiency and STH efficiency are $\pm 1.67\%$,
297 $\pm 1.82\%$ and $\pm 3.49\%$, respectively. It can be seen that a maximum sunlight to hydrogen (STH)
298 efficiency of 18% is recorded for the developed CPV-hydrogen system, which is about 2 times
299 higher than the electrical efficiency of conventional PV modules. In the morning, with the increase
300 in the DNI, the STH efficiency is increasing. However, after certain limit, further increase in DNI
301 is cause drop in the STH efficiency. This trend can be explained with the maximum efficiency
302 curve for CPV system. The CPV efficiency was increasing in the morning with increase in the
303 DNI, due to increase in the concentration at the cell area. However, with further increase in the
304 DNI, the efficiency slightly drops due to increase in the cell temperature at higher concentration,
305 as explained above in Fig. 6. The CPV efficiency stabilizes at 24-25% while STH efficiency

306 remains steady at 15%. However, if electrolyser efficiency curve is observed, a continuous drop
307 can be seen during first half of the day when DNI is increasing and a continuous increase occurs
308 during other half of the day when DNI start to drop in the afternoon. With increase in the DNI,
309 the power output of CPV also increases as there is a slight drop in the efficiency and consequently,
310 the electrical power delivered to the electrolyser also increases, causing increase in the voltage
311 and current of the electrolyser, as shown in Fig. 8. With continuous increase in the operating
312 voltage of electrolyser, its efficiency drops continuously, as the efficiency only depends upon the
313 operating voltage. However, when DNI starts to drop in the afternoon, the CPV power and
314 electrolyser voltage drop as well, causing an increase in the efficiency of electrolyser.

315 From the system performance curves, it can be seen that a lot of parameters are simultaneously
316 affecting the system performance. Thus, the true system performance cannot be rated by
317 maximum power output or efficiency only because the real field conditions change throughout the
318 day. For operation of the system like CPV, especially in the urban region with tropical weather
319 where the system can only respond to beam part of solar radiations, the feasibility of such a system
320 can only be justified with average real field performance instead of instantaneous maximum
321 efficiency. Therefore, to analyse the feasibility of CPV-hydrogen system in tropical weather
322 conditions, the system output was monitored for many days, under different weather conditions.
323 Fig. 9 shows the daily average STH efficiency for different days with different amount of received
324 beam radiations. It can be seen that with the increase in the amount of beam radiation received per
325 day, the daily average STH efficiency is decreasing. The main cause for this drop is similar to the
326 one given for Fig. 6 and Fig. 8 where efficiency of the system is decreasing with the increase in
327 the DNI. The first reason is due to increase in the cell temperature with increase in DNI or
328 concentration. However, the second reason is the drop in the electrolyser efficiency due to increase
329 in its operating voltage which increases with increase in the power output. Such trend can be
330 explained through Fig. 10 which shows the variation of hydrogen production rating with increase
331 in the amount of received radiations. The hydrogen production rating is increasing with increase
332 in the solar energy input i.e. for clear days. This increase in hydrogen production rating, on the
333 other hand, depicts the lower electrolyser efficiency, as explained in Fig. 11. It can be seen that
334 for higher rating or power consumption, the electrolyser efficiency is decreasing. These results of
335 decreasing efficiency suggest to operate electrolyser cell at lower power or voltage. For larger
336 production, multiple electrolyser cells can be connected in series for better system efficiency. The
337 above charts does not encourage the operation of CPV-hydrogen systems in region with low DNI
338 availability. In fact, these results show the feasible operation of CPV-hydrogen system even in the
339 tropical region.

340 From this series of experiments, it can be seen that the system showed an average long term STH
341 efficiency of 15%. This efficiency is 1.5-2 times higher than the instantaneous electrical efficiency
342 of conventional PV. In addition, the electrolyser showed average efficiency in the range of 66-
343 70% with hydrogen production rating of 47-50 kWh/kg. The CPV-hydrogen system showed an
344 average production rating of 217 kWh/kg.

345 From the plant designer's point of view, the presented average performance data is very important
346 to estimate the actual size of the system for the production requirement. It has been shown that the
347 maximum rated performance does not reflect the actual field potential as the system output is

348 continuously changing during field operation. The field conditions vary throughout the day and
349 so as the system output. Therefore, the average long term performance gives the correct estimation
350 of system output for the real field operation. Based upon the solar beam radiations availability,
351 one can easily estimate the average hydrogen production rating and so as the electrolyser
352 efficiency. This can give the average STH efficiency which can be used to calculate the system
353 size or area, for the certain hydrogen production requirement. In addition, these full day
354 experiments also validates the accuracy and performance of the developed compact two axis solar
355 tracking system. This also shows the excellent performance and accuracy of the developed solar
356 tracking sensor.

357 **5. Conclusion**

358 A compact CPV-hydrogen system has been successfully designed and developed for the rooftop
359 application. The microcontroller based hybrid two axis solar tracking system has been developed
360 for economical but highly accurate operation of the compact CPV field. A novel design of the
361 solar tracking sensor has also been proposed for the cost effective operation, with high accuracy.
362 The double collimator based solar tracking sensor showed tracking error sensitivity of as high as
363 0.1° , same as the accuracy of the commercially available solar tracking sensors for CPV
364 application, but at a fraction of the cost. The main reason for such high accuracy at low cost is due
365 to the development of optical based design of solar tracking sensor with ordinary photosensors,
366 instead of utilizing highly sensitive photosensor based design with high cost. The developed CPV
367 system showed stable operation at the rooftop, with required tracking accuracy throughout the
368 days during long term operation. Moreover, the performance and production of developed CPV-
369 hydrogen system is also tested and evaluated for tropical weather conditions. A maximum of 18%
370 STH efficiency was recorded for the CPV based hydrogen production system. Daily average
371 efficiency of 15% was recorded with STH production rating of 217 kWh/kg. This shows that
372 despite only being responsive to the beam radiations, CPV system is still feasible for the operation
373 in tropical region, with superior performance than the conventional PV.

374 Such proposed compact CPV system design will offer the same application scope to the CPV
375 technology, as that of conventional PV system but with higher efficiency. In addition, a highly
376 efficient sustainable hydrogen production system will be in the reach of every common customer
377 that will help for the better utilization of solar energy with high power density, at any time,
378 throughout the day.

379 **6. Acknowledgement**

380 This research was supported by the International Research Scholarship of Mechanical
381 Engineering Department, National University of Singapore and collaborated with King
382 Abdullah University of Science and Technology.

383 **Nomenclature**

STH	Sunlight to Hydrogen	PEM	Proton Exchange Membrane
d	Distance between photo-sensors (mm)	h	Distance between collimator and photo-sensor array (mm)

ω	Hour angle (degree)	δ	Declination angle (degree)
θ_a	Azimuth angle (degree)	θ_z	Zenith angle (degree)
DNI	Direct Normal Irradiance, (W/m^2)	A_{con}	Area of Solar Concentrator (m^2)
PSD	Position Sensitive Diode	b_t	Collimated beam thickness (mm)
I_E	Electrolyser Current (A)	S	Distance between collimating lenses (mm)
MJC	Multi-junction solar cell	CPV	Concentrated Photovoltaic
PV	Photovoltaic	GHI	Global horizontal irradiance
f_{cx}	Focal length of convex lens (mm)	f_{cn}	Focal length of concave lens (mm)
D_{cx}	Convex lens diameter (mm)	ϕ	Latitude (degree)
ADC	Analogue to Digital Converter	CTS	Colour Tracking Sensor
RTC	Real Time Clock	GPS	Global positioning system
N_{EC}	Number of Cells of Electrolyser	V_{CPV}	CPV Voltage (V)
I_E	Electrolyser Current (A)	η_{EL}	Electrolyser Efficiency (%)
\dot{n}_{E,H_2}	Hydrogen Production Flow Rate from Electrolyser (mol/s)	η_{EF}	Faraday Efficiency of Electrolyser (%)
η_{CPV}	CPV Efficiency (%)	P_{CPV}	CPV Power Output (W)
n_E	Electrons Requirement for Water Splitting	η_{CPV_H2}	Sunlight to Hydrogen (STH) Efficiency for CPV (%)
η_{PV}	PV Efficiency (%)	η_{PV_H2}	Sunlight to Hydrogen (STH) Efficiency for PV (%)
U_E	Electrolyser Cell Voltage (V)	F	Faraday Constant (A.s/mol)
MPPT	Maximum Power Point Tracking	I_{CPV}	CPV Current (A)

384 7. References

- 385 [1] Tehrani SS, Saffar-Avval M, Mansoori Z, Kalhori SB, Abbassi A, Dabir B, Sharif M.
386 Development of a CHP/DH system for the new town of Parand: An opportunity to mitigate
387 global warming in Middle East. *Applied Thermal Engineering* 2013, **59(1)**, 298-308.
- 388 [2] Bengtsson P, Eikevik T. Reducing the global warming impact of a household heat pump
389 dishwasher using hydrocarbon refrigerants. *Applied Thermal Engineering* 2016, **99**, 1295-302.
- 390 [3] Ozden E, Tari I. Energy–exergy and economic analyses of a hybrid solar–hydrogen
391 renewable energy system in Ankara, Turkey. *Applied Thermal Engineering* 2016, **99**, 169-78.
- 392 [4] Seifi H, Sadrameli SM. Improvement of renewable transportation fuel properties by
393 deoxygenation process using thermal and catalytic cracking of triglycerides and their methyl
394 esters. *Applied Thermal Engineering* 2016, **100**, 1102-10.
- 395 [5] Li MJ, Zhao W, Chen X, Tao WQ. Economic analysis of a new class of vanadium redox-
396 flow battery for medium-and large-scale energy storage in commercial applications with
397 renewable energy. *Applied Thermal Engineering* 2017, **114**, 802-14.
- 398 [6] Rasid MM, Murata J, Takano H. Fossil fuel cost saving maximization: Optimal allocation
399 and sizing of Renewable-Energy Distributed Generation units considering uncertainty via
400 Clonal Differential Evolution. *Applied Thermal Engineering* 2017, **114**, 1424-32.

- 401 [7] Ascione F, Bianco N, De Masi RF, De Stasio C, Mauro GM, Vanoli GP. Multi-objective
402 optimization of the renewable energy mix for a building. *Applied Thermal Engineering* 2016,
403 **101**, 612-21.
- 404 [8] Burhan M, Oh SJ, Chua KJ, Ng KC. Solar to hydrogen: Compact and cost effective CPV
405 field for rooftop operation and hydrogen production. *Applied Energy* 2017, **194**, 255-66.
- 406 [9] Burhan M, Oh SJ, Chua KJE, Ng KC. Double lens collimator solar feedback sensor and
407 master slave configuration: Development of compact and low cost two axis solar tracking
408 system for CPV applications. *Solar Energy* 2016, **137**, 352-363.
- 409 [10] Burhan M, Chua KJE, Ng KC. Long term hydrogen production potential of concentrated
410 photovoltaic (CPV) system in tropical weather of Singapore. *International Journal of*
411 *Hydrogen Energy* 2016, **41(38)**, 16729-16742.
- 412 [11] Burhan M, Chua KJE, Ng KC. Electrical rating of concentrated photovoltaic (CPV)
413 systems: long-term performance analysis and comparison to conventional PV systems.
414 *International Journal of Technology* 2016, **7(2)**, 189-196. DOI: 10.14716/ijtech.v7i2.2983.
- 415 [12] Kong H, Hao Y, Wang H. A solar thermochemical fuel production system integrated with
416 fossil fuel heat recuperation. *Applied Thermal Engineering* 2016, **108**, 958-66.
- 417 [13] Burhan M, Shahzad MW, Ng KC. Development of performance model and optimization
418 strategy for standalone operation of CPV-hydrogen system utilizing multi-junction solar cell.
419 *International Journal of Hydrogen Energy* 2017, [http://dx.doi.org/
420 10.1016/j.ijhydene.2017.08.186](http://dx.doi.org/10.1016/j.ijhydene.2017.08.186)
- 421 [14] Burhan M, Chua KJE, Ng KC. Sunlight to hydrogen conversion: Design optimization and
422 energy management of concentrated photovoltaic (CPV-Hydrogen) system using micro genetic
423 algorithm. *Energy* 2016, **99**, 115-128.
- 424 [15] Muhammad B, Seung JO, Ng KC, Chun W. Experimental Investigation of Multijunction
425 Solar Cell Using Two Axis Solar Tracker. In *Applied Mechanics and Materials* 2016 (Vol.
426 819, pp. 536-540). Trans Tech Publications.
- 427 [16] Burhan M., Chua KJE, Ng KC. Simulation and development of a multi-leg homogeniser
428 concentrating assembly for concentrated photovoltaic (CPV) system with electrical rating
429 analysis. *Energy Conversion and Management* 2016, **116**, 58-71.
- 430 [17] Burhan M, Shahzad MW, Ng KC. Long-term performance potential of concentrated
431 photovoltaic (CPV) systems. *Energy Conversion and Management* 2017, **148**, 90-9.
- 432 [18] Mathur SS, Negi BS, Kandpal TC. Geometrical designs and performance analysis of a
433 linear fresnel reflector solar concentrator with a flat horizontal absorber. *International journal*
434 *of energy research* 1990, **14(1)**, 107-24.

- 435 [19] Horne S, Conley G, Gordon J, Fork D, Meada P, Schrader E, Zimmermann T. A solid 500
436 sun compound concentrator PV design. In *Photovoltaic Energy Conversion, Conference*
437 *Record of the 2006 IEEE 4th World Conference 2006*, **1**, 694-697.
- 438 [20] Garboushian V, Stone KW, Slade A. 12 The Amonix High-Concentration Photovoltaic
439 System. *Concentrator Photovoltaics 2007*, **130**, 253.
- 440 [21] David FK, Stephen HJ. Laminated solar concentrating photovoltaic device. US Patent
441 application publication; 2007. p. US2007/0256726.
- 442 [22] McConnell R. A Solar Concentrator Pathway to Low-Cost Electrolytic Hydrogen. *Solar*
443 *Hydrogen Generation 2008*, 65-86.
- 444 [23] International Energy Agency (IEA). Trends 2015 in Photovoltaic Applications, Survey
445 Report of Selected IEA Countries between 1992 and 2014. Report IEAPVPS T1-27; 2015.
- 446 [24] BURHAN M. THEORETICAL AND EXPERIMENTAL STUDY OF
447 CONCENTRATED PHOTOVOLTAIC (CPV) SYSTEM WITH HYDROGEN
448 PRODUCTION AS ENERGY STORAGE. (Doctoral dissertation); 2015.
- 449 [25] Agbossou K, Kolhe M, Hamelin J, Bose TK. Performance of a stand-alone renewable
450 energy system based on energy storage as hydrogen. *IEEE Transactions on energy Conversion*
451 2004, **19(3)**, 633-40.
- 452 [26] Wang Z, Roberts RR, Naterer GF, Gabriel KS. Comparison of thermochemical,
453 electrolytic, photoelectrolytic and photochemical solar-to-hydrogen production technologies.
454 *International journal of hydrogen energy 2012*, **37(21)**, 16287-301.
- 455 [27] EVWorld. Energy content of fuels,
456 <http://www.evworld.com/library/energy_numbers.pdf>, [Date retrieved: 20-12-2015].
- 457 [28] ForestBioEnergy. Sustainable forestry for bioenergy and biobased products. Energy
458 basics. Fact Sheet 5.8, <[http://www.forestbioenergy.net/trainingmaterials/fact-sheets/module-](http://www.forestbioenergy.net/trainingmaterials/fact-sheets/module-5-fact-sheets/fact-sheet-5-8-energy-basics)
459 [5-fact-sheets/fact-sheet-5-8-energy-basics](http://www.forestbioenergy.net/trainingmaterials/fact-sheets/module-5-fact-sheets/fact-sheet-5-8-energy-basics)>. [Date retrieved: 20-12-2015].
- 460 [29] Abdallah K, Nijmeh S. Two axes sun tracking system with PLC control. *Energy*
461 *Conversion and Management 2004*, **45(11-12)**, 1931-1939.
- 462 [30] Xu G, Zhong Z, Wang B, Guo R, Tian Y. Design of PSD based solar direction sensor.
463 In *Sixth International Symposium on Precision Mechanical Measurements 2013*, 89162K-
464 89162K. International Society for Optics and Photonics.
- 465 [31] Lin-Heng L, Lok-Ming C, Chia A, Gunawansa A, Harn-Wei K. Sustainability Matters,
466 Challenges and Opportunities in Environmental Management in Asia. Pearson Education
467 South Asia Pte Ltd, 2011. Singapore.

- 468 [32] Khaselev O, Bansal A, Turner JA. High-efficiency integrated multijunction
469 photovoltaic/electrolysis systems for hydrogen production. *International Journal of Hydrogen*
470 *Energy* 2001, **26(2)**, 127-132.
- 471 [33] Oh SJ, Burhan M, Ng KC, Kim Y, Chun W. Development and performance analysis of a
472 two-axis solar tracker for concentrated photovoltaics. *International Journal of Energy*
473 *Research* 2015, **39(7)**, 965-76.

474 **List of Figure Captions:**

475 Figure 1: Schematic Scope of CPV-Hydrogen System

476 Figure 2: Design Schematic of Compact CPV System with Double Lens Collimator based Solar
477 Tracking Sensor

478 Figure 3: Design Schematic of Control Box for Compact CPV System

479 Figure 4: Developed Prototype of Compact CPV-Hydrogen System for Rooftop Operation

480 Figure 5: Flow Schematic of Developed Compact CPV-Hydrogen System

481 Figure 6: Maximum Performance characteristics of Developed Compact CPV System

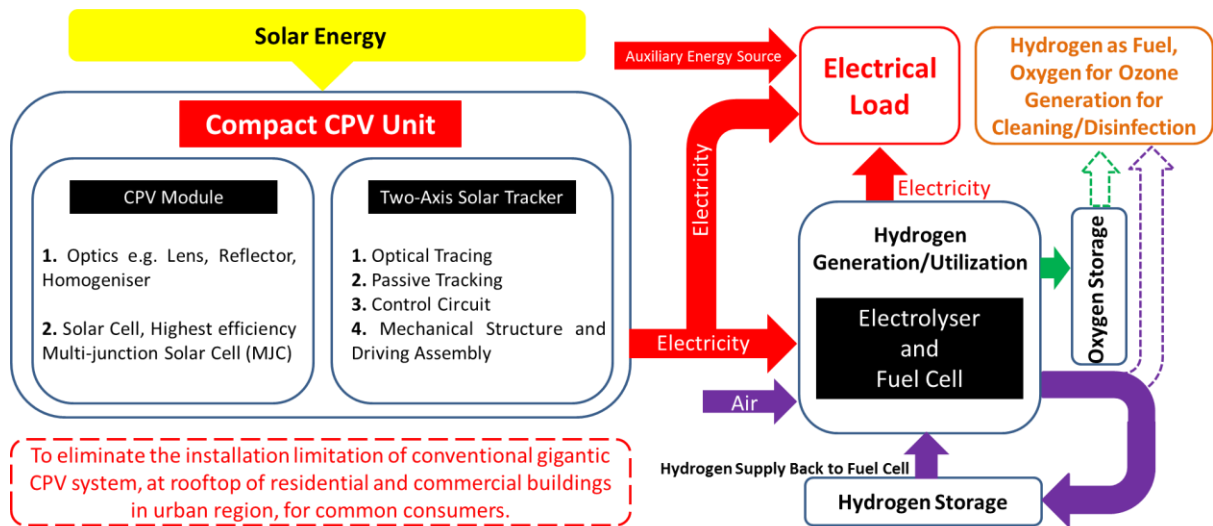
482 Figure 7: Performance Characteristics of PEM Electrolyser

483 Figure 8: Performance Curves for Compact CPV-Hydrogen System during Whole Day Operation

484 Figure 9: Variation of Daily Average STH efficiency against Daily Received Solar Energy for
485 CPV-Hydrogen System

486 Figure 10: Variation of Daily Average Hydrogen Production Rating against Daily Received Solar
487 Energy for CPV-Hydrogen System

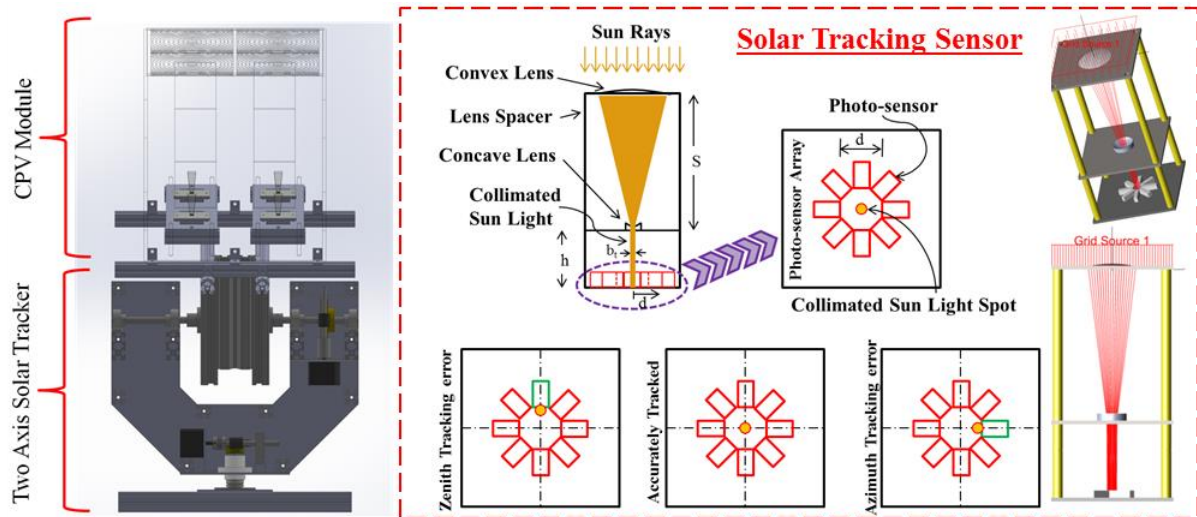
488 Figure 11: Variation of Daily Average Hydrogen Production Rating against Daily Average
489 Electrolyser Efficiency for CPV-Hydrogen System



490

491

Figure 1: Schematic Scope of CPV-Hydrogen System

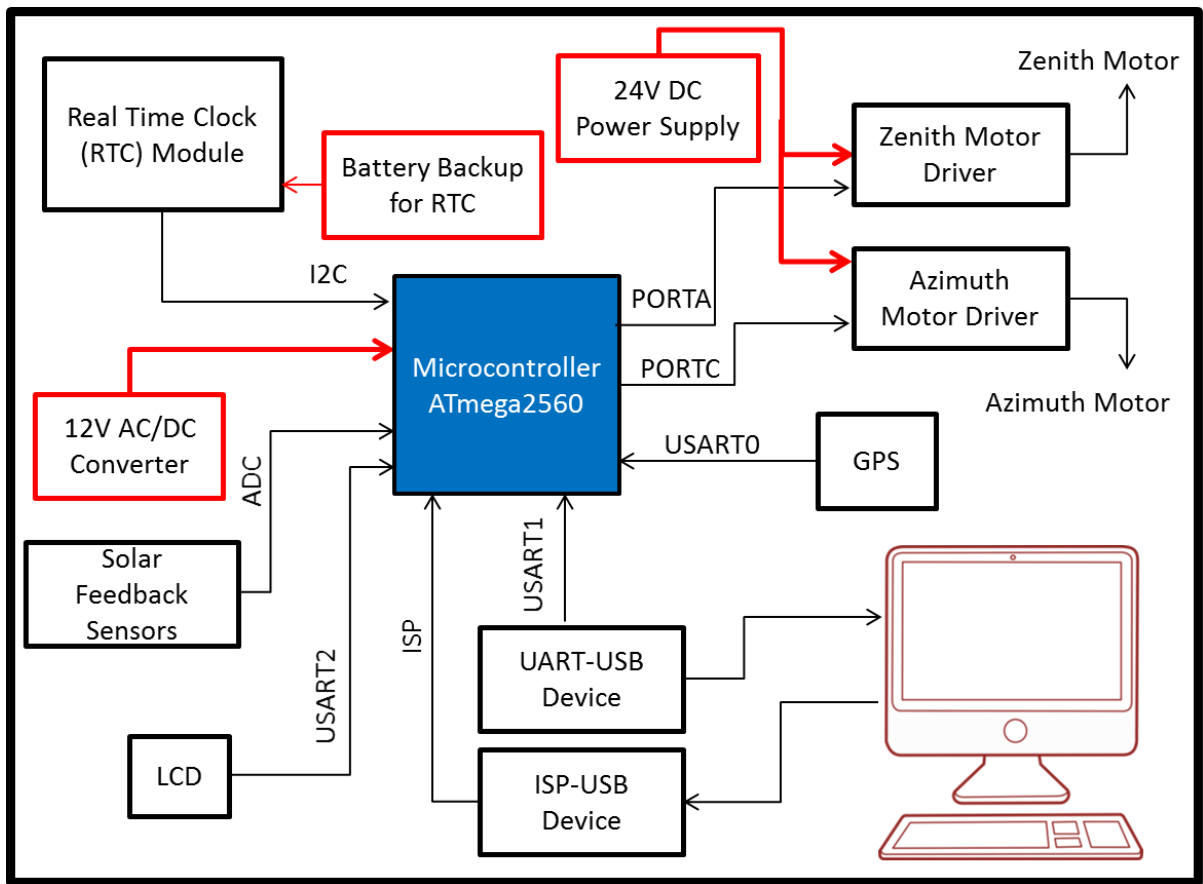


492

493

494

Figure 2: Design Schematic of Compact CPV System with Double Lens Collimator based Solar Tracking Sensor



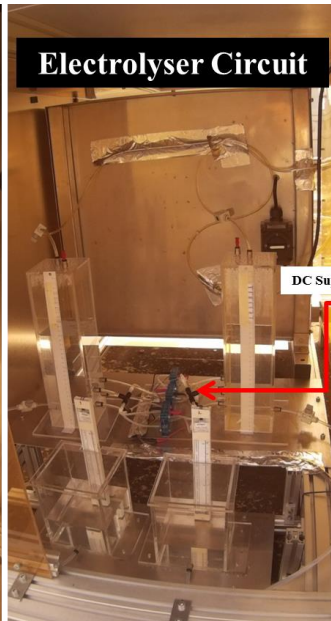
495

496

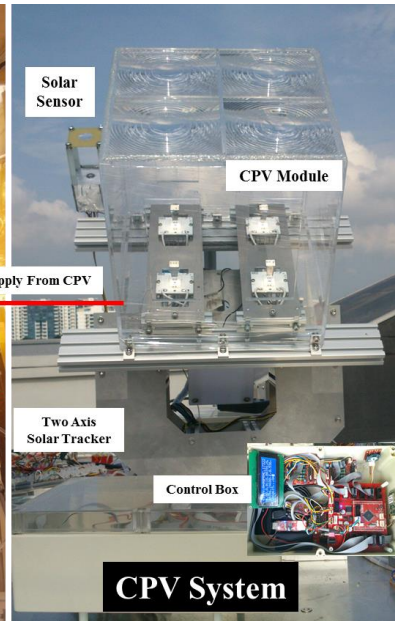
Figure 3: Design Schematic of Control Box for Compact CPV System



Hydrogen Compression Unit



Electrolyser Circuit



Solar Sensor

CPV Module

DC Supply From CPV

Two Axis Solar Tracker

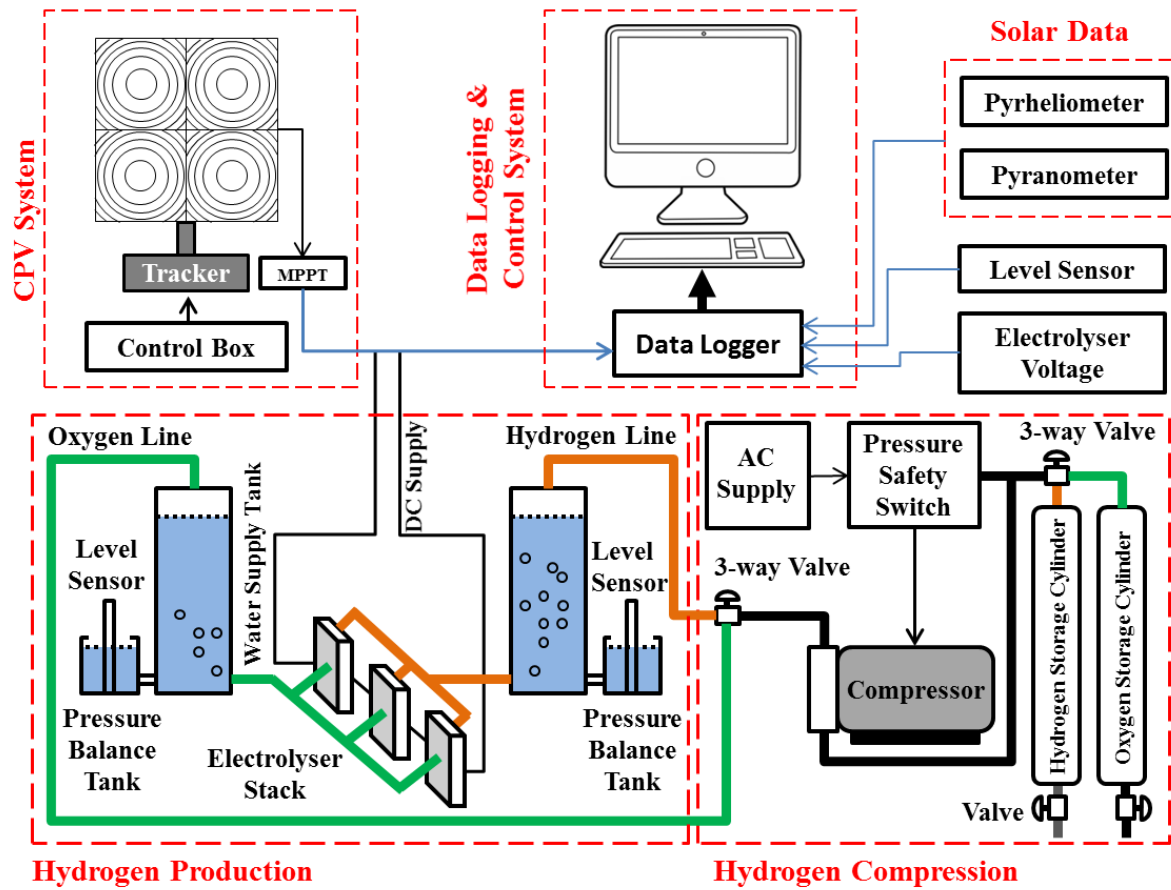
Control Box

CPV System

497

498

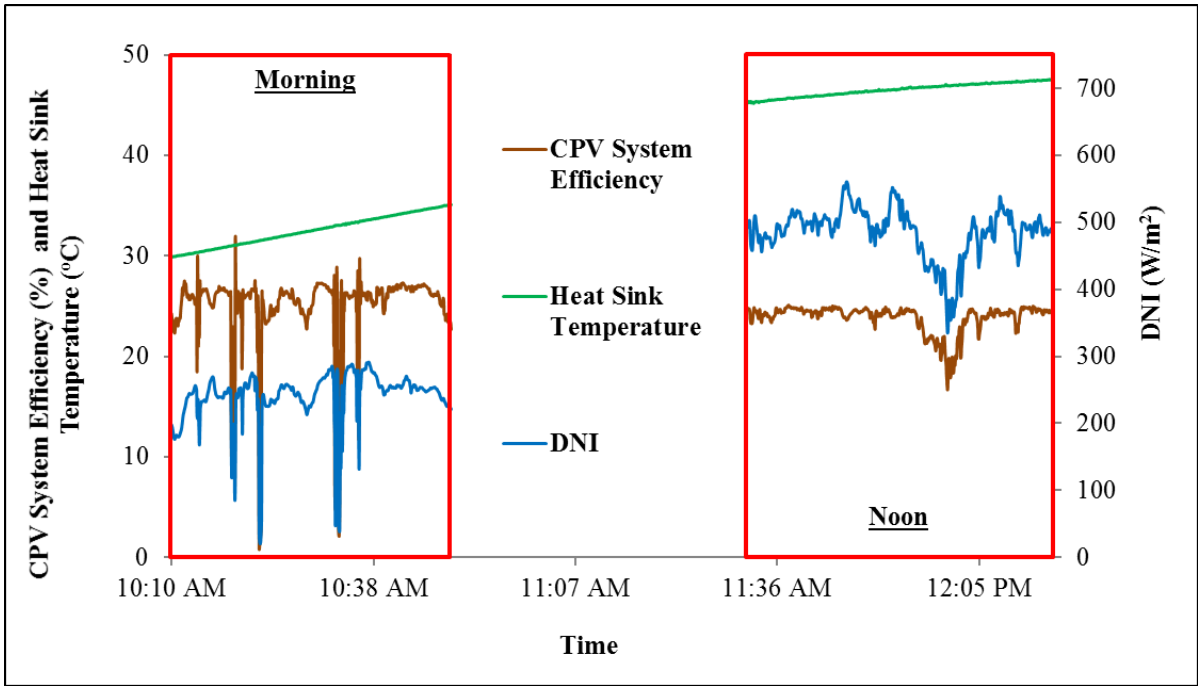
Figure 4: Developed Prototype of Compact CPV-Hydrogen System for Rooftop Operation



499

500

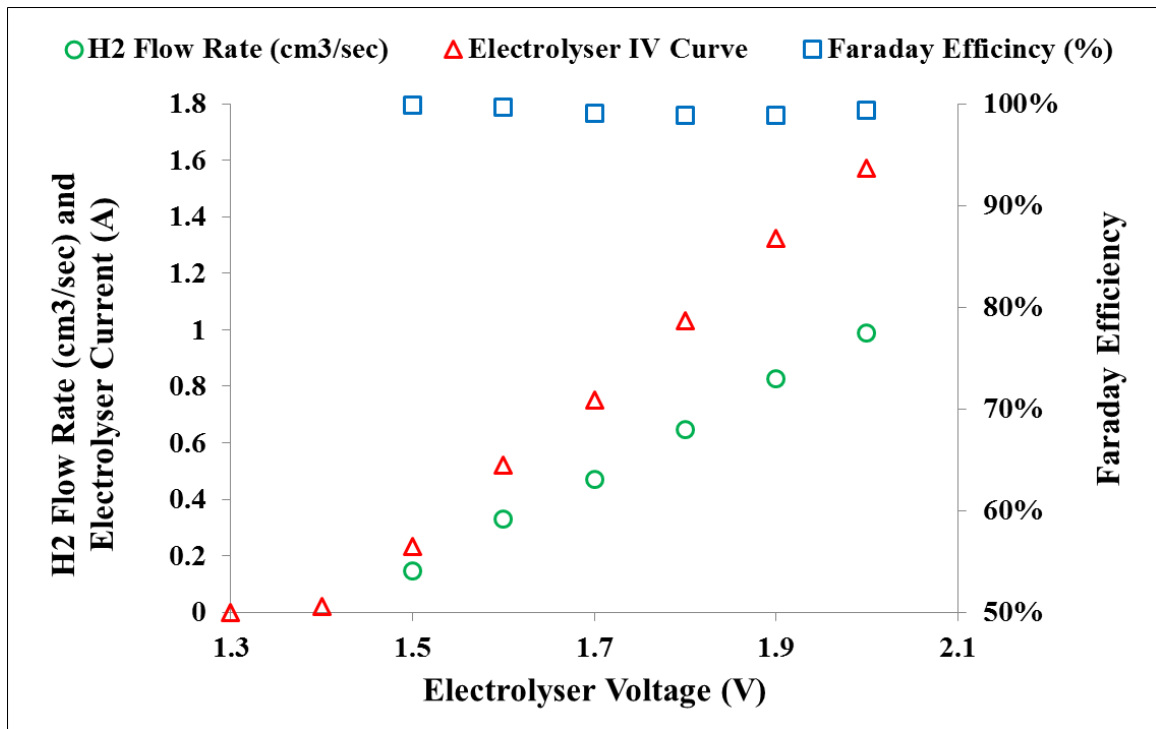
Figure 5: Flow Schematic of Developed Compact CPV-Hydrogen System



501

502

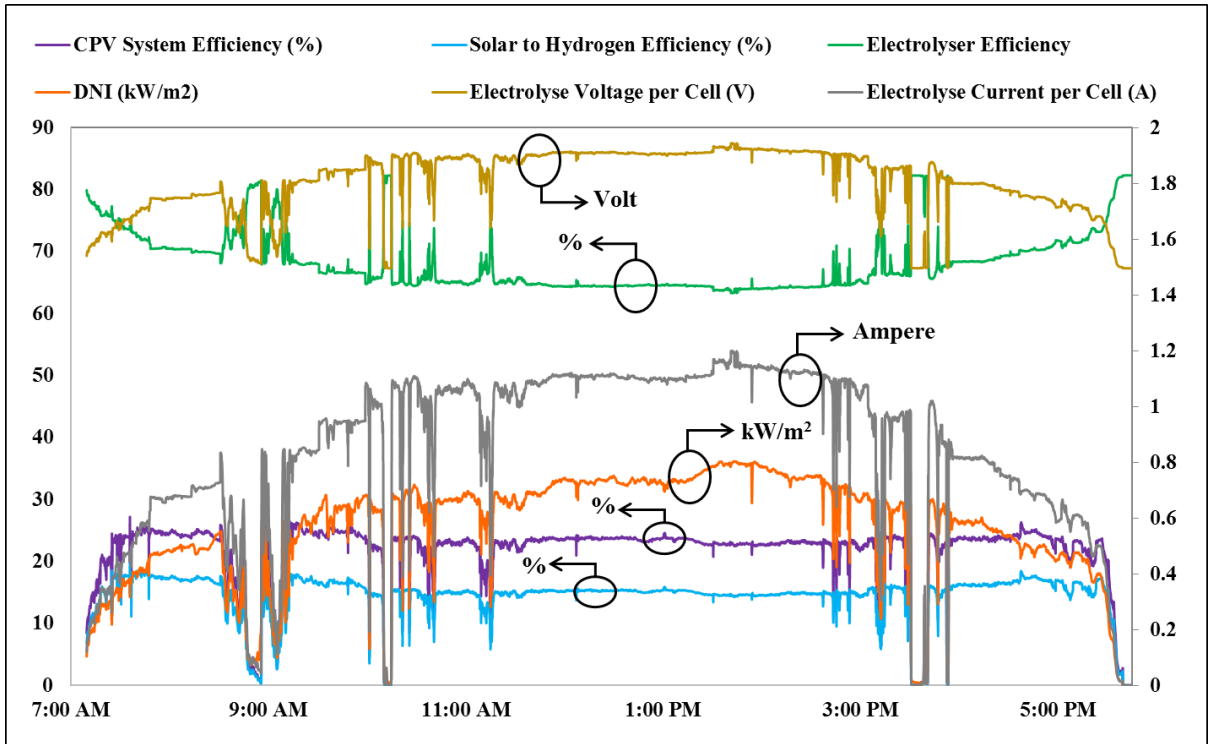
Figure 6: Maximum Performance characteristics of Developed Compact CPV System



503

504

Figure 7: Performance Characteristics of PEM Electrolyser

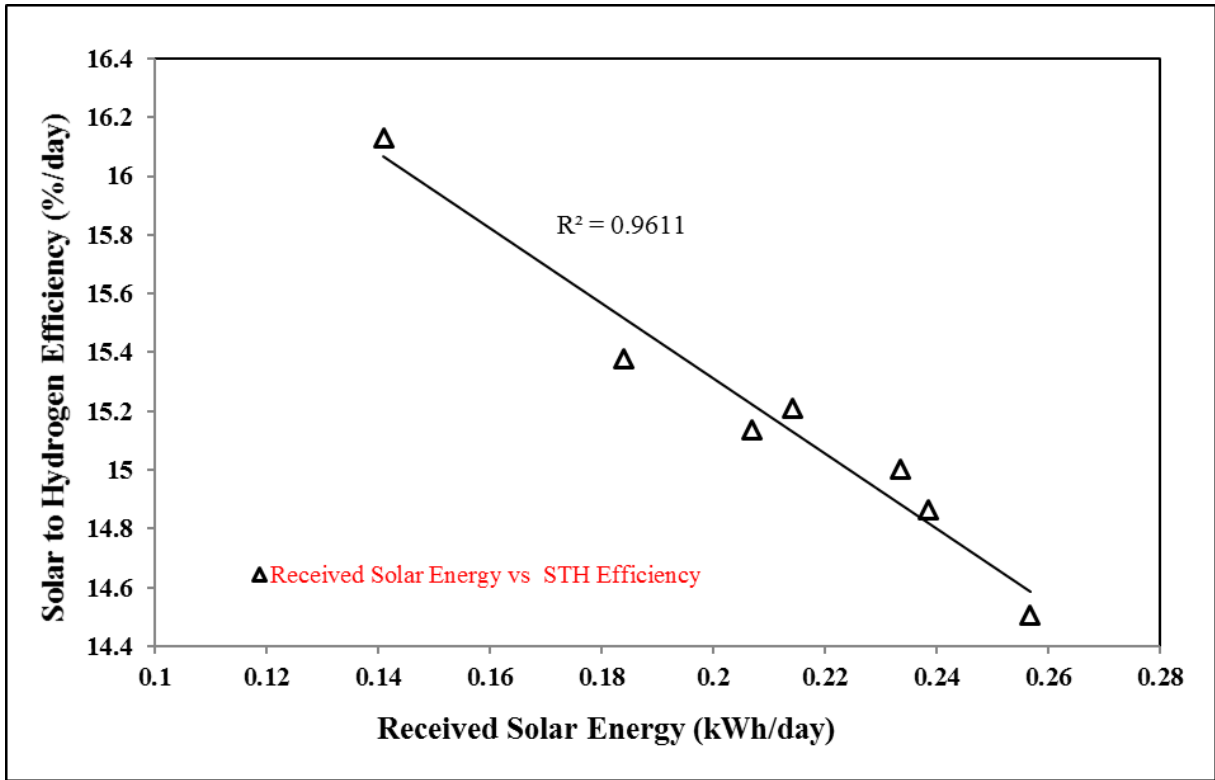


505

506

507

Figure 8: Performance Curves for Compact CPV-Hydrogen System during Whole Day Operation

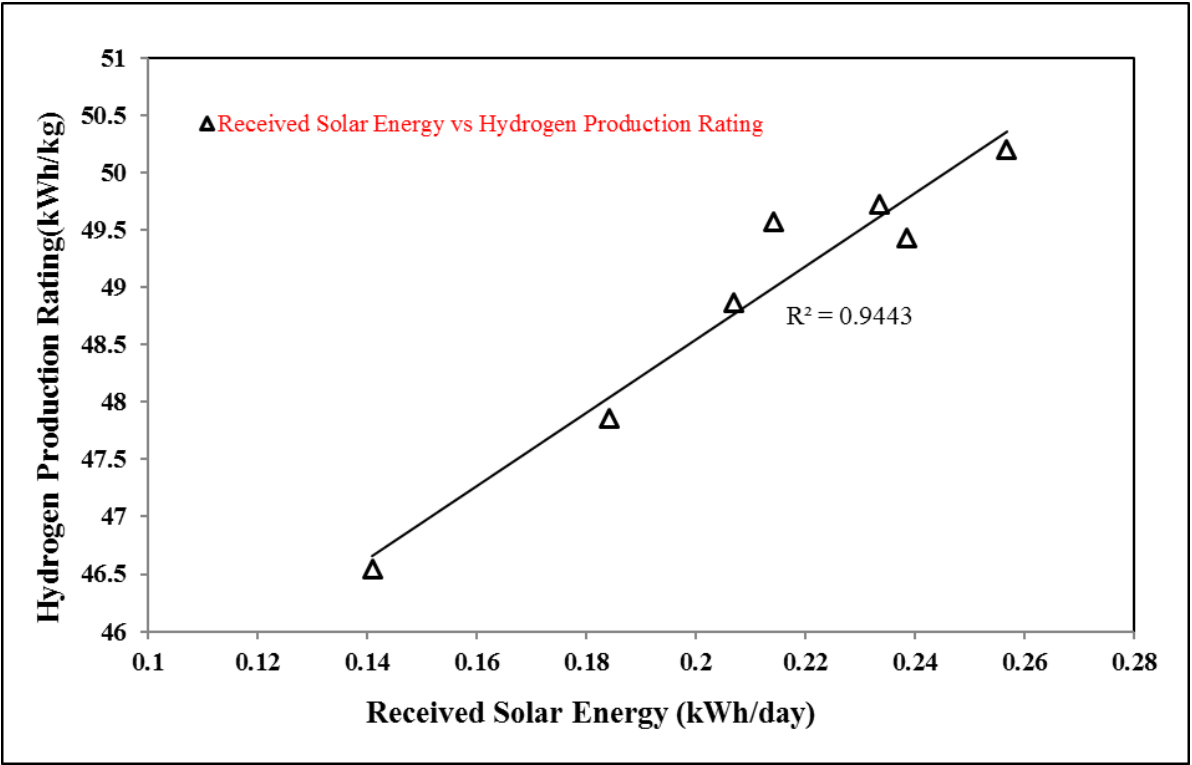


508

509

510

Figure 9: Variation of Daily Average STH efficiency against Daily Received Solar Energy for CPV-Hydrogen System

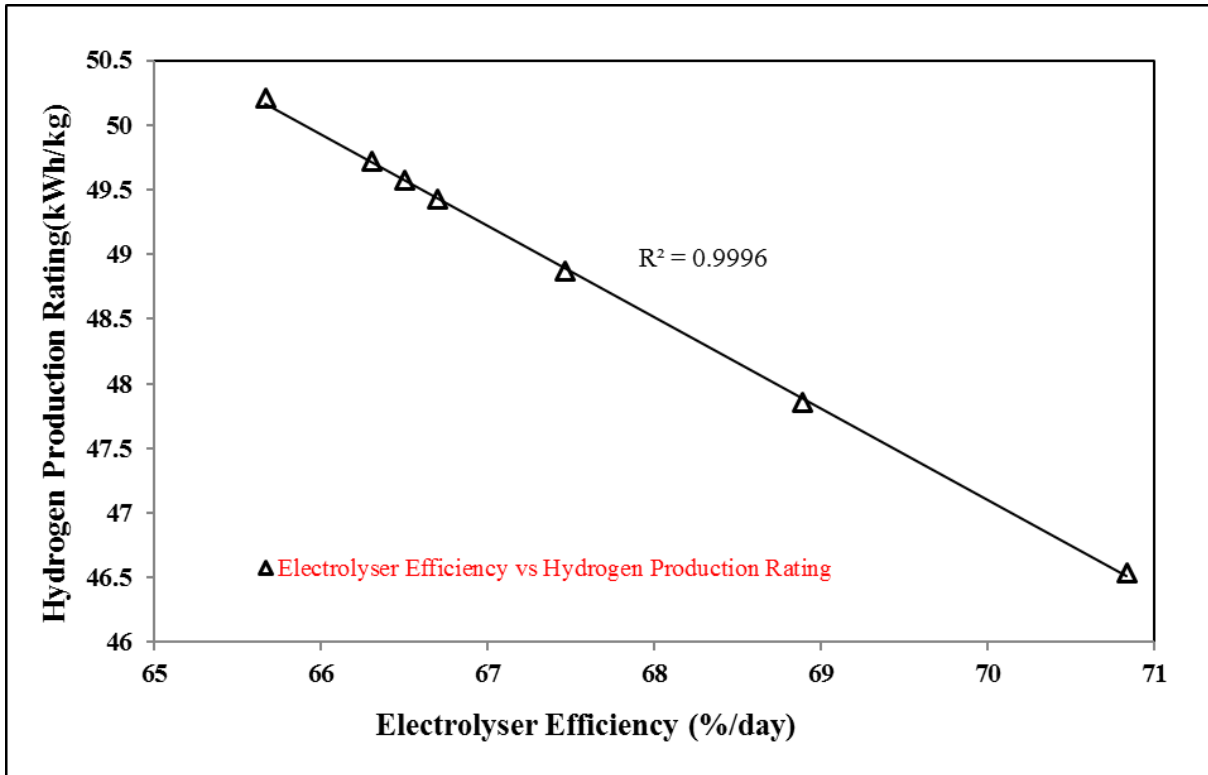


511

512

513

Figure 10: Variation of Daily Average Hydrogen Production Rating against Daily Received Solar Energy for CPV-Hydrogen System



514

515 Figure 11: Variation of Daily Average Hydrogen Production Rating against Daily Average
 516 Electrolyser Efficiency for CPV-Hydrogen System

517